

Advancing Multi-Organ Disease Care: A Hierarchical Multi-Agent Reinforcement Learning Framework

Daniel Jason Tan

djtan@u.nus.edu

National University of Singapore
Singapore, Singapore

Qianyi Xu

e0673214@u.nus.edu

National University of Singapore
Singapore, Singapore

Dilruk Perera

dilruk@nus.edu.sg

National University of Singapore
Singapore, Singapore

Kay Choong See

kaychoongsee@nus.edu.sg

National University of Singapore
Singapore, Singapore

Mengling Feng

ephfm@nus.edu.sg

National University of Singapore
Singapore, Singapore

Abstract

In healthcare, multi-organ system diseases pose unique and significant challenges as they impact multiple physiological systems concurrently, demanding complex and coordinated treatment strategies. Despite recent advancements in the AI based clinical decision support systems, these solutions only focus on individual organ systems, failing to account for complex interdependencies between them. This narrow focus greatly hinders their effectiveness in recommending holistic and clinically actionable treatments in the real world setting. To address this critical gap, we propose a novel Hierarchical Multi-Agent Reinforcement Learning (HMARL) framework. Our architecture deploys specialized and dedicated agents for each organ system and facilitates inter-agent communication to enable synergistic decision-making across organ systems. Furthermore, we introduce a dual-layer state representation technique that contextualizes patient conditions at both global and organ-specific levels, improving the accuracy and relevance of treatment decisions. We evaluate our HMARL solution on the task of sepsis management, a common and critical multi-organ disease, using both qualitative and quantitative metrics. Our method learns effective, clinically aligned treatment policies that considerably improve patient survival. We believe this framework represents a significant advancement in clinical decision support systems, introducing the first RL solution explicitly designed for multi-organ treatment recommendations. Our solution moves beyond prevailing simplified, single-organ models that fall short in addressing the complexity of multi-organ diseases.

CCS Concepts

• **Applied computing** → **Health informatics**; • **Information systems** → **Decision support systems**.

Permission to make digital or hard copies of all or part of this work for personal or classroom use is granted without fee provided that copies are not made or distributed for profit or commercial advantage and that copies bear this notice and the full citation on the first page. Copyrights for components of this work owned by others than the author(s) must be honored. Abstracting with credit is permitted. To copy otherwise, or republish, to post on servers or to redistribute to lists, requires prior specific permission and/or a fee. Request permissions from permissions@acm.org.
Conference acronym 'XX, Woodstock, NY

© 2018 Copyright held by the owner/author(s). Publication rights licensed to ACM.
ACM ISBN 978-1-4503-XXXX-X/2018/06
<https://doi.org/XXXXXXX.XXXXXXX>

Keywords

Healthcare AI, Clinical Decision Support, Dynamic Treatment Regimes, Reinforcement Learning, Personalized Medicine

ACM Reference Format:

Daniel Jason Tan, Qianyi Xu, Dilruk Perera, Kay Choong See, and Mengling Feng. 2018. Advancing Multi-Organ Disease Care: A Hierarchical Multi-Agent Reinforcement Learning Framework. In *Proceedings of Make sure to enter the correct conference title from your rights confirmation email (Conference acronym 'XX)*. ACM, New York, NY, USA, 11 pages. <https://doi.org/XXXXXXX.XXXXXXX>

1 Introduction

Multi-organ diseases are characterized by the sequential or simultaneous impairment of multiple organs [1]. They present significant challenges in clinical management due to the difficulty in balancing therapeutic trade-offs, and their potential for life-threatening outcomes. Treating these diseases requires a holistic approach that accounts for interdependencies between different organ systems [23]. Existing guideline-based approaches treat organs in isolation and rely on one-size-fits-all recommendations [25]. A recent example is COVID-19, which primarily affects the respiratory system, but could also lead to dysfunction in the immune, nervous, and gastrointestinal systems [2, 20]. Another example is sepsis, a serious condition resulting from the body's dysregulated response to infection. Sepsis can lead to widespread inflammation, coagulation abnormalities, and metabolic disruptions, cascading into multi-organ dysfunction [4].

Recent advances in reinforcement learning (RL), have shown promise in optimizing clinical decision-making for complex diseases. Its capacity to learn adaptive policies from high-dimensional, complex data makes it a powerful tool for such tasks. Notably, deep RL has been applied to sepsis treatment, to learn dynamic treatment regimes (DTRs) from electronic health records (EHRs) of intensive care unit (ICU) patients [9]. Subsequent work has explored model-free approaches, such as Dueling Double Deep Q-Networks (D3QN) [16, 26] and model-based approaches [17]. RL has also been applied to chronic diabetes management [13, 24, 28]. Despite the multi-organ nature of many major diseases, existing RL approaches have predominantly focused on recommending treatments targeting a single organ system at a time. For example, current solutions for sepsis primarily address the cardiovascular system via fluids and vasopressor dosing optimization [9, 12, 16]. This is a significant

limitation, as treatments for one organ can significantly influence the efficacy or safety of treatments for another. For example, recommending vasopressors (VAs) to stabilize blood pressure can increase renal impairment for a patient with concurrent renal dysfunction [27]. While solutions with explicit consideration of multiple organ systems exist, their primary focus has been diagnosis, instead of complex treatment recommendation [7, 8].

Multi-organ disease treatment recommendation introduces complexities beyond what traditional RL and non-RL-based recommendation solutions can effectively manage. For example, as the number of organ systems or treatments increase, the number of combinations of actions increases exponentially, making action spaces untenable for standard single-agent RL algorithms to navigate. Additionally, patients' measured physiological variables will relate to each organ system's unique physiology in different ways, adding an additional layer of complexity that a multi-organ solution must account for. Consequently, there is a clear need to develop a robust and holistic treatment recommendation solution tailored for multi-organ system disease management.

We propose a hierarchical multi-agent RL (HMARL) solution, which divides the complex task of multi-organ treatment recommendation among a hierarchy of specialized sub-agents. Each agent operates within its own localized state and action spaces, simplifying decision-making and allowing agents to focus exclusively on relevant subspaces. Carefully designed inter- and intra-agent communication mechanisms enable collaboration when necessary, alleviating the burden on individual agents and leading to more efficient training and faster convergence. Moreover, understanding patient states and their dynamics within localized contexts is essential for accurate treatment recommendations. For example, when treating the cardiovascular system, more focus should be on factors such as ejection fraction and cardiac enzyme levels, whereas renal treatments require attention to factors such as glomerular filtration rate and electrolyte balances [3]. To achieve this, we propose a multi-layer hierarchical representation technique that first captures broad health indicators at the root level and then refines them into organ-specific representations, which are utilized by the corresponding agents at these levels. Collectively, this HMARL system, combined with the multi-layer hierarchical representation technique, effectively manages the complexities of multi-organ treatment recommendation.

We summarize our main contributions as follows:

- To the best of our knowledge, we propose the first-of-its-kind multi-organ treatment recommendation solution.
- We introduce a compact HMARL framework that decomposes the complex task of multi-organ disease management into manageable subtasks, handled by specialized sub-agents operating within localized state and action spaces, independently and collaboratively.
- We develop a multi-layer hierarchical representation technique that learns broad and specific patient representations, tailored to treatment context, aiding accurate decision-making at multiple levels.

- We demonstrate the effectiveness of our approach through extensive experiments, showing its superiority over traditional RL models in handling multi-organ interdependencies and improving treatment outcomes.

Our offline RL-based solution is trained and tested on retrospective public data as is standard in healthcare RL to ensure safety and stability. The solution serves purely as a clinical decision support system that offers data-driven treatment recommendations as an expert-in-the-loop solution. There are no ethical violations in its development or use.

2 Methodology

2.1 Hierarchical Decomposition

Complex decision-making tasks such as treatment recommendation or distributed control involves complex interaction among multiple subsystems or decision domains. They often contain large combinatorial action spaces, contextual dependencies and the need for local specialization with global coordination. To address these challenges, we propose a general hierarchical MARL framework that decomposes the overall problem into multiple payers of specialized decision makers (agents). Each layer addresses a different abstraction enabling a scalable, interpretable and modular policy learning.

2.1.1 HMARL Framework Overview: Proposed HMARL framework is organized as follows. At the highest level, a root agent selects broad high-level options or task branches. These options invoke intermediate coordinator agents that manage related subtasks within specialized domains or scopes. Leaf level sub agents are responsible for fine-grained decisions such as selecting specific actions to perform within their specialized action subspaces. Importantly, we include both intra-branch (local) and inter-branch (global) communications modules to share key information to coordinate decisions across boundaries, where necessary. This hierarchical decomposition help reduce the burden on individual agents through smaller manageable scopes and supports structured collaboration through communication pathways and shared latent representations. The framework is flexible, supporting both independent and cooperative training regimes, and scalable to complex and heterogeneous action spaces (i.e., discrete, continuous and hybrid).

2.1.2 Scalability and Complexity: Consider a decision problem with N treatment dimensions (e.g., organ or treatment modality), each with a local action space \mathcal{A}_i of size $|\mathcal{A}_i| = k$. A standard flat RL agent operates on the full joint space $\mathcal{A} = \prod_{i=1}^N \mathcal{A}_i$, resulting in an exponential decision complexity of $\mathcal{O}(k^N)$. In contrast, proposed hierarchical MARL framework decomposes this problem across a hierarchy of depth d , where decisions are made sequentially by specialized agents. At each layer, an agent selects from at most k options. Some agents (e.g., mixture agents) may invoke up to b sub-agents in parallel to gather auxiliary recommendations. Under this setting, the per-episode decision complexity is reduced to $\mathcal{O}(d \cdot b \cdot k)$ (see Figure 1a). This formulation assumes conditional branching, where only relevant sub-agents are activated. If each agent (or layer) addresses on average \bar{m} decision dimensions, the minimum hierarchy depth satisfies $d \geq \lceil \frac{N}{\bar{m}} \rceil$, with $b \leq \min(d, N)$.

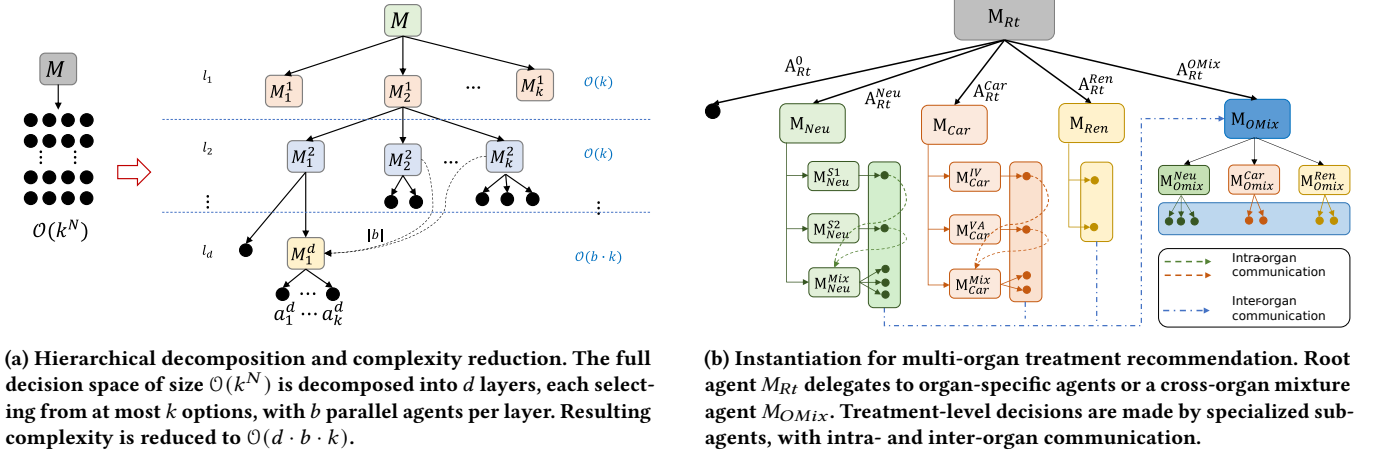


Figure 1: Hierarchical multi-agent framework and its medical instantiation. (a) A generic HMARL framework achieves scalable decision-making via depth-wise decomposition. (b) Specific application to multi-organ treatment recommendation with coordinated agent behavior.

Theoretically, d could linearly scale with N yet it is substantially smaller in practice. For example, in our instantiation below with $N = 6$ treatment dimensions, a depth of $d = 3$ is sufficient, as the decision space is structured around natural clinical groupings. Even in the worst-case scenario ($d = N$), complexity is $\mathcal{O}(N \cdot b \cdot k)$, which is polynomial and far more tractable than the exponential complexity. Moreover, each agent operates within a localized subspace $\mathcal{A}_i \subset \mathcal{A}$ and exclusively trained on relevant samples. This reduces gradient interference from unrelated subtasks, improves sample efficiency, and mirrors real-world collaborative clinical practice. The architecture supports plug-and-play extensibility. New treatment modalities or decision dimensions can be integrated by adding new agents without retraining the full hierarchy, allowing the overall system to scale gracefully with added complexity.

2.1.3 Clinical Use Case: Proposed HMARL framework is domain-agnostic and can generate multiple decompositions for a given task, with varied effectiveness based on the selected hierarchy and communication pathways. Guided by our clinical collaborators, we instantiate the framework analogous to a coordinated team of medical specialists and supervisors at practice. The model considers seven treatments across three organs (see Figure 1b). This decomposition restricts each subtask to a defined subspace, significantly reducing the decision making complexity while enabling selective coordination when necessary.

At the top level, the root agent M_{Rt} selects one of five high-level options: No-treatment (\mathcal{A}_{Rt}^0), Neuro-only (\mathcal{A}_{Rt}^{Neu}), Cardio-only (\mathcal{A}_{Rt}^{Car}), Renal-only (\mathcal{A}_{Rt}^{Ren}), or Organ mixture (\mathcal{A}_{Rt}^{OMix}). Using the commonly selected *no-treatment* option at this level reduces the burden on downstream agents by pruning unnecessary branches early and reducing overall action space. When an organ-specific action is selected, the corresponding domain-level agent (i.e., M_{Neu} , M_{Car} , or M_{Ren}) is invoked. Neuro and Cardio agents operate similarly where each chooses between individual treatments (i.e., S1 or S2 for Neuro; IV or Vaso for Cardio) or a mixture, invoking

subsequent sub-agents to recommend treatment dosages. Intra-organ communication is used for treatment mixtures (\mathcal{A}_{Neu}^{Mix} , \mathcal{A}_{Car}^{Mix}) to effectively aggregate recommendations from respective single-treatment sub-agents, enhancing local coordination. In contrast, the Renal agent M_{Ren} directly selects among four diuretic levels or dialysis, as treatment mixing is not applicable. Multi-organ decisions (\mathcal{A}_{Rt}^{OMix}) are taken by the coordinator agent M_{OMix} using the inter-organ communication to obtain their treatment recommendations, reducing the need to learn these from scratch. Accordingly, it invokes a combination of sub-agents (M_{OMix}^{Neu} , M_{OMix}^{Car} , M_{OMix}^{Ren}), each of which incorporates relevant signals from the other domains. For instance, M_{OMix}^{Neu} considers recommendations from Cardio and Renal sub-agents. This cross-communication allows agents to adjust outputs to account for interactions, streamlining coherent multi-organ plans. Agents are trained only on samples drawn from their respective action subspaces to improve efficiency and minimize interference. For example, M_{Car}^{IV} learns from IV-only cases, while M_{Car}^{Mix} is trained on samples where both IV and Vaso were used.

This instantiation reflects a real-world clinical setting where a lead physician delegates to specialists. The resulting hierarchy decomposes decision-making across dedicated and mixture agents, enabling scalable inter- and intra-organ coordination. This task-specific decomposition and structured communication protocols supports modular policy learning making it highly applicable to broader multi-organ treatment scenarios.

2.2 RL Components

2.2.1 States: Accurate patient understanding is essential for effective multi-organ treatment recommendations, as it requires integrating complex interdependencies of physiological features and organ functions. Therefore, we propose a hierarchical patient representation approach that acknowledges the varying significance of raw features at different analytical levels.

At the root level, *Unified State Representations* are learned to extract broad health indicators and their dynamics, providing a

foundational understanding of patients. This representation is used for broader decision-making at the root level, and sets the stage for subsequent, more granular recommendations. At the organ levels, they are refined to learn *Targeted State Representations*, tailored to unique physiological requirements and interrelationships of specific organs. For instance, in cardiac treatments, the embeddings prioritize ejection fraction and cardiac enzyme levels, capturing cardiac health indicators. In contrast, renal treatments focus on glomerular filtration rate and electrolyte balances, assessing renal function. This approach ensures that organ-specific recommendations are precise and relevant.

This dual-layer hierarchical representation strategy balances broad applicability with detailed specificity, enhancing decision-making considering each organ's condition. It comprises of the following levels:

Unified State Representations: Inspired by the representation learning proposed in [15] we learn the unified representations as follows. Each patient at time t is represented by their raw d -dimensional feature, $x_t = \{x_{t,1}, x_{t,2}, \dots, x_{t,d}\} \in \mathbb{R}$ (for details on x_t , see Appendix Section *Feature Processing*). At the root agent level, these features are transformed using dense latent embeddings $E^{Rt} = \{e_1^{Rt}, e_2^{Rt}, \dots, e_d^{Rt}\} \in \mathbb{R}^{d \times k}$. Each k -dimensional latent embedding vector $e_i^{Rt} \in \mathbb{R}^k$ transforms its corresponding raw feature into a more informative dense latent representation. The resultant patient-specific embeddings are represented as $F_t^{Rt} = \{f_{t,1}^{Rt}, f_{t,2}^{Rt}, \dots, f_{t,d}^{Rt}\} \in \mathbb{R}^{d \times k}$, where $f_{t,i}^{Rt} = (x_{t,i} \cdot e_i^{Rt})$. These latent embeddings e_i^{Rt} are generic at the root agent level, providing a holistic understanding of the patient by transforming each feature into a homogeneous latent space. The vector $f_{t,i}^{Rt}$ denotes the transformed representation specific to the patient at time t .

To capture the complex interdependencies among these features, a higher-order interaction layer is introduced. This layer computes the element-wise product between all pairs of embeddings in F_t^{Rt} resulting an interaction matrix $G_t^{Rt} \in \mathbb{R}^{k \times d(d+1)/2}$. Final output of the layer consists of first- and second- order interactions, denoted by $H_t^{Rt} = (F_t^{Rt} \parallel G_t^{Rt})$, which is then aggregated via sum pooling to generate an observation vector as $o_t^{Rt} = \sum_{l=1}^{d(d+3)/2} H_{t,l}^{Rt} \in \mathbb{R}^k$.

Moreover, given the importance of patient trajectory information for understanding the patient's current context, a temporal contextual state vector c_t^{Rt} . This vector captures the recent history of the patient's states by applying an exponential decay to the previous observation vectors, resulting in $c_t^{Rt} = \sum_{i=t-3}^{t-1} e^{-(t-i)} o_i^{Rt} \in \mathbb{R}^k$.

The final core-state vector at the root level at time t is constructed by concatenating the current observation vector o_{Rt} with the temporal contextual state vector c_{Rt} , resulting in $s_t^{Rt} = (o_t^{Rt} \parallel c_t^{Rt}) \in \mathbb{R}^{2k}$. This vector is learned end-to-end during the training of the root agent, enabling the model to capture immediate and historical physiological measurements effectively. The reduced dimensionality to $2k$ in the dense space also simplifies the complexity of subsequent decision-making processes.

Targeted State Representations: The generic latent embeddings E^{Rt} learned at the root level are fine-tuned to generate targeted (organ-level) state representations that reflect unique characteristics and critical features relevant to each organ. Accordingly, we transform the raw features x_t using specialized latent embeddings

E^{Neu} , E^{Car} and E^{Ren} , to obtain organ-specific state representations s_t^{Neu} , s_t^{Car} and s_t^{Ren} . They are used as input states for training the corresponding sub-agents (M_{Neu} , M_{Car} and M_{Ren}). A concatenated targeted state representation $s_t^{OMix} = [s_t^{Neu} \parallel s_t^{Car} \parallel s_t^{Ren}]$ is used to train organ mixture agents (M_{OMix} , M_{OMix}^{Neu} , M_{OMix}^{Car} and M_{OMix}^{Ren}), ensuring they are trained on a comprehensive representation of all organs.

2.2.2 Actions. In addition to the agent options discussed above for higher-level agents, this section provides detailed information on the actions of leaf-level agents. According to our hierarchical task decomposition approach, each agent operates within a factored action space. This helps reduce the learning burden on each agent and prevents the effects of potentially low-quality samples across subspaces. Based on clinical expertise and data availability, we selected six treatments. Two for each the Cardiovascular system: IV fluids (IV) and vasopressors (Vaso), Neuro system: anesthetics (S1) and analgesics (S2), and Renal system: diuretics and dialysis. These organ systems and their respective treatments were chosen by a physician according to clinical priority in intensive care patients. Each treatment plays a unique and critical function within its biological system and requires careful control to ensure efficacy and safety. Our framework is scalable to any number of organ systems and treatments. The proposed hierarchy is generic which allows integration of agents operating on continuous and discrete action spaces. However, we tested the approach using discrete action spaces. Dosages for each treatment were discretized into five levels (no-action + 4 quantiles), except dialysis, which is a binary action (active or inactive). Proposed hierarchy supports mixing of any treatment within or across systems, aligning with common clinical practices derived from our data analysis and clinical consultations. For example, we enforced exclusive use of one renal treatment at a time—either diuretics or dialysis, and allowed all other treatment combinations. This showcases the hierarchy's adaptability to incorporate such domain specific constraints. Accordingly, our solution flexibly handles organ systems with different degrees of complexity and configurations of actions, enabling the effectiveness of the solution in real, complex clinical settings.

2.2.3 Reward Function. We used a hybrid reward system, combining a mortality-based terminal reward—positive (+ R) for survival, and negative (− R) for death—with clinically guided intermittent rewards to adjust rewards based on immediate health outcomes. Specifically, we define intermediate rewards based on changes in the Sequential Organ Failure Assessment (SOFA) score and blood lactate levels—two validated surrogates of physiological deterioration. The reward penalizes both persistently high SOFA scores and increases in SOFA or lactate between successive time steps, while assigning positive reward for improvements. The overall form is:

$$R(s_t, s_{t+1}) = \begin{cases} +R, & \text{if } s_{t+1} \in \mathcal{S}_T \cap \mathcal{S}_{sur} \\ -R, & \text{if } s_{t+1} \in \mathcal{S}_T \cap \mathcal{S}_{dec} \\ R_{im}(s_t, s_{t+1}), & \text{if } s_{t+1} \notin \mathcal{S}_T \end{cases} \quad (1)$$

$$R_{im}(s_t, s_{t+1}) = C_0(s_{t+1}^{SOFA} = s_t^{SOFA} \wedge s_{t+1}^{SOFA} > 0) + C_1(s_{t+1}^{SOFA} - s_t^{SOFA}) + C_2 \tanh(s_{t+1}^{lactate} - s_t^{lactate}) \quad (2)$$

where $C_0 = -0.025$, $C_1 = -0.125$, and $C_2 = -2$. The tanh term ensures that large lactate swings do not disproportionately affect learning.

The chosen approach addresses the challenges of credit assignment and reward sparsity in long sequences. They ensure that immediate health improvements are reflected in decision-making while supporting adaptable, cross-organ policy learning applicable across diverse healthcare settings. Our reward design follows established structures in healthcare RL research; however our framework itself is generalizable as it is not tied to a specific reward function. Where terminal rewards suffice, our framework can operate without intermittent rewards.

2.3 Q Learning

Traditional RL frameworks, using Markov Decision Processes (MDPs), often assume actions are executed instantaneously and have uniform durations. This simplifies modeling, but fails to capture real-world complexities with actions spanning multiple steps and varying duration.

Therefore we utilize an integration of an options framework with semi-MDPs and decentralized MDPs within a structured hierarchical system. This approach enables an agent to invoke options that ranges from primitive (one-step) to extended (multiple-step) actions at any point. Then the agent regains control to initiate another option only after the previous one completes. Accordingly, the traditional action-value function is adapted to an option-value function $Q^\pi(s, o)$ which indicates the value of invoking option o in state s under a policy π . This is defined as the expected sum of discounted future rewards:

$$Q^\pi(s, o) = \mathbb{E}\{r_{t+1} + \gamma r_{t+2} + \gamma^2 r_{t+3} + \dots \mid \epsilon^\pi(o, s, t)\}$$

where γ is a discount factor and $\epsilon^\pi(o, s, t)$ is the execution of option o in state s from time t to its termination. Unlike the standard options framework, our solution contains independent and cooperative agents controlling options (see Section 2.1). Thus, root level Q-values are updated as follows:

$$Q(s, o) \leftarrow Q(s, o) + \alpha [Q_{tgt}(s, o) - Q(s, o)] \quad (3)$$

where $Q_{tgt}(s, o)$ is determined based on the controlling agent and the option o as follows:

$$Q_{tgt}(s, o) = \begin{cases} r, & \text{if } o = A_{Rt}^0 \\ \max_{a \in A_{Neu}} Q_{Neu}(s, a), & \text{if } o = A_{Rt}^{Neu} \\ \max_{a \in A_{Car}} Q_{Car}(s, a), & \text{if } o = A_{Rt}^{Car} \\ \max_{a \in A_{Ren}} Q_{Ren}(s, a), & \text{if } o = A_{Rt}^{Ren} \\ \max_{a \in A_{OMix}} Q_{OMix}(s, a), & \text{if } o = A_{Rt}^{OMix} \end{cases}$$

where r is the immediate reward for selecting no-action A_{Rt}^0 , A_{Neu} , A_{Car} , A_{Ren} and A_{OMix} are the action spaces for Neuro, Cardio, Renal agents, and their combined action space $A_{Neu} \times A_{Car} \times$

A_{Ren} . Value functions $Q_{Neu}(s, a)$, $Q_{Car}(s, a)$, and $Q_{Ren}(s, a)$ for corresponding agents are updated using Temporal Difference (TD) learning as follows:

$$\begin{aligned} Q_{Neu}(s, a) &\leftarrow Q_{Neu}(s, a) + \alpha [y^{Neu} - Q_{Neu}(s, a)] \\ Q_{Car}(s, a) &\leftarrow Q_{Car}(s, a) + \alpha [y^{Car} - Q_{Car}(s, a)] \\ Q_{Ren}(s, a) &\leftarrow Q_{Ren}(s, a) + \alpha [y^{Ren} - Q_{Ren}(s, a)] \end{aligned} \quad (4)$$

where $y^X = r + \gamma \max_{a'} Q_X(s', a'; \theta^-)$ for $X \in \{Neu, Car, Ren\}$ are TD targets computed from target networks with parameters θ^- . The Q values for each system are updated using observed rewards and estimated values of the next state (s').

M_{OMix} is trained using the QMix architecture [18], combining individual value functions of its sub-agents (M_{OMix}^{Neu} , M_{OMix}^{Car} , and M_{OMix}^{Ren}) into a unified value function (Q_{OMix}). QMix supports cooperative training and consistent decision-making across agents by enforcing a monotonicity constraint. The constraint keeps the weights of the mixing network non-negative, ensuring that the $\arg\max$ operation on Q_{OMix} is consistent with those from the sub-agents. Hence, Q_{OMix} is represented as follows:

$$\arg\max_{a \in A_{OMix}} Q_{OMix}(s, a) = \begin{pmatrix} \arg\max_{a_{OMix}^{Neu} \in A_{OMix}^{Neu}} Q_{OMix}^{Neu}(s_{OMix}^{Neu}, a_{OMix}^{Neu}) \\ \arg\max_{a_{OMix}^{Car} \in A_{OMix}^{Car}} Q_{OMix}^{Car}(s_{OMix}^{Car}, a_{OMix}^{Car}) \\ \arg\max_{a_{OMix}^{Ren} \in A_{OMix}^{Ren}} Q_{OMix}^{Ren}(s_{OMix}^{Ren}, a_{OMix}^{Ren}) \end{pmatrix} \quad (5)$$

where $s_{OMix}^{Neu} = [s_t^{OMix}, a_{Car}, a_{Ren}]$ concatenates the targeted state representation and communicated dosage outputs (a_{Car} and a_{Ren}) from the opposite organ-specific agents (M_{Car} and M_{Ren}) as described under *Hierarchical Decomposition*. s_{OMix}^{Car} and s_{OMix}^{Ren} are formed analogously.

2.3.1 Training Process: We used a two phase approach to train the proposed hierarchical model (see *Algorithm 1* in Appendix). In phase one, the root agent (M_{Rt}) is trained first. Resulting latent embeddings E^{Rt} are then fine-tuned during the subsequent training of organ-specific agents (M_{Neu} , M_{Car} , and M_{Ren}). In the process, targeted embeddings (E^{Neu} , E^{Car} and E^{Ren}) are learned and formulate *Targeted State Representations*. These representations are used to train the corresponding lower-level sub-agents. Independent agents directly learn Q values from received rewards (see Equation 4), whereas cooperative agents M_{OMix}^{Neu} , M_{OMix}^{Car} , M_{OMix}^{Ren} are trained using shared rewards (Equation 5). In phase two, we integrate the full hierarchy by using the trained organ-specific agents from phase one. $Q(s, a)$ values from these agents are used to retrain M_{Rt} (see Equation 3), and no other agent is retrained. After training, at each timestep, M_{Rt} evaluates the patient state s_t^{Rt} and select either *no-action*, or invokes lower level agents for final treatment and dosage recommendations.

3 Experiments

3.1 Datasets

We collected data on 30,440 patients under Sepsis-3 criteria from the popular MIMIC-IV database [6]. The data spans from 24 hours pre-diagnosis to 48 hours post-diagnosis forming a maximum 72 hour window per patient, barring death or ICU discharge. We defined a continuous state-space which included 44 physiological measurements including vital signs, laboratory test results, severity scores and demographics. State and actions data were aggregated into four-hourly windows to generate uniform patient data sequences. The patient trajectories were randomly split into 75% training and 25% testing sets. Additionally, we collected data for 4,390 sepsis patients from the AmsterdamUMC dataset [22] to conduct an external validation of our trained models using the same set of state and action variables. High level statistics of the cohorts are listed in Table 1. See Appendix, Section *RL Actions* and *RL States* for more information on the state and action spaces.

Table 1: Cohort characteristics for MIMIC-IV and AmsterdamUMC

Dataset	Cohort	% Female	Age (Mean)	ICU LOS (Mean)	Population
MIMIC-IV	Overall	42.11	66.14	5d 4h	30,440
	Non-Survivors	44.00	69.77	6d 12h	4,948
	Survivors	41.75	65.44	4d 22h	25,492
AmsterdamUMC	Overall	38.82	61.71	7d 8h	4,390
	Non-Survivors	39.49	66.64	9d 9h	961
	Survivors	38.63	60.33	6d 18h	3,429

3.2 Baselines

We evaluated our model performance against multiple baselines, including single- (D3QN-S and SoftAC-S) and multi-agent systems under independent (D3QN-O) and cooperative (QMIX-O and QMIX-T) learning approaches:

- **Clinician:** Policy derived from clinician’s recorded action trajectories in the test set.
- **Single D3QN (D3QN-S)** [16]: Single-agent D3QN predicting all treatment and dosage combinations in a flattened action space. We used the original implementation with tuned hyperparameters.
- **Single SoftAC (SoftAC-S)** [5]: A single-agent Soft Actor-Critic predicting all action combinations in a flattened action space. We used the original implementation and tuned hyperparameters.
- **Organ-specific D3QN (D3QN-O):** Three independent D3QN agents for Neuro, Cardio and Renal systems. Models are trained using all available samples, including those treated exclusively for the target organ and those mixed with other organ treatments. Averaged quantitative metrics are reported.
- **Treatment-specific D3QN (D3QN-T):** Five independent D3QN agents for S1, S2, IV, vaso, and diuretics/dialysis. Models are trained using all available samples, including those using single-treatments and mixed-treatments. Averaged quantitative metrics are reported.

Table 2: Policy Evaluation on MIMIC-IV and AmsterdamUMC

Policy	MIMIC-IV		External Validation	
	V	Mortality (%)	V	Mortality (%)
Clinician	9.08	16.27	7.74	21.89
SoftAC-S	-3.26	20.52 \pm 0.68	-6.22	28.59 \pm 0.85
D3QN-S	-1.29	19.79 \pm 0.77	-6.87	29.13 \pm 0.92
D3QN-O	12.74	14.57 \pm 0.30	8.01	20.57 \pm 0.50
D3QN-T	13.05	13.62 \pm 0.43	10.24	19.91 \pm 0.45
QMIX-O	15.45	13.29 \pm 0.37	8.70	20.12 \pm 0.55
QMIX-T	17.16	12.74 \pm 0.30	11.07	18.56 \pm 0.46
Proposed	21.73	9.95 \pm 0.33	12.95	17.34 \pm 0.43

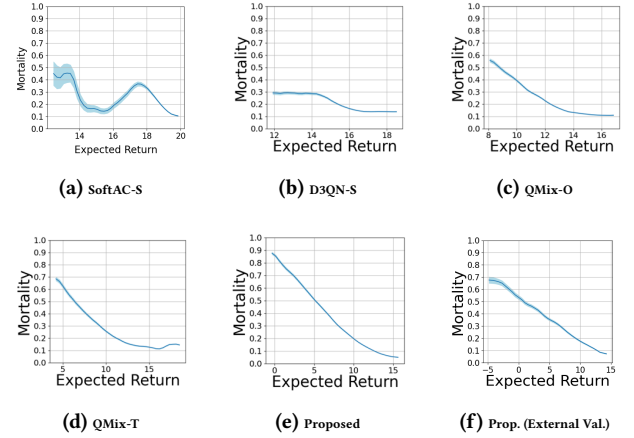


Figure 2: Mortality vs. expected return for all models. The shaded area represents standard errors.

- **Organ-coordinated QMIX (QMIX-O):** Trained end-to-end with three cooperative agents, each corresponding to an organ system operating exclusively within its factored action spaces. Predicts treatments across organs by cooperation, using a QMIX mixing network.
- **Treatment-coordinated QMIX (QMIX-T):** Uses five cooperative treatment-level agents (S1, S2, IV fluids, vasopressors, diuretics/dialysis), learning cooperatively via a QMIX network.

All models used the same state representations, action discretization methods, and reward functions. All codes for data processing and model training are included in the supplementary materials and will publicly available upon acceptance.

3.3 Results and Discussion

We present and discuss our experimental results as answers to four key research questions as follows.

3.3.1 RQ1: Does the proposed solution effectively learns a superior treatment policy? We evaluate the performance of learned policies using off-policy quantitative and qualitative metrics (see Table 2). They do not require a simulator, but adopt a well-established approach using offline learning on retrospective data. These metrics, widely used in healthcare RL enable safe, effective

learning from clinical outcomes without real-time exploration risks [9, 16].

1) *Average Returns*: We use Consistent Weighted Per-Decision Importance Sampling (CWPDIS), a standard OPE method to estimate expected returns from each policy V^{CWPDIS} (V). [21]. A higher V corresponds to a more effective policy. Both single agent baselines (D3QN-S and SoftAC-S) result in negative average returns. This indicates the single agent systems' inability to learn effective policies in this complex setting. Meanwhile, the multi-agent model QMix-T was the best performing baseline according to OPE returns. This suggests that for our particular multi-organ problem, MARL approaches with some form of cross-agent communication can be beneficial for policy learning. Overall, our model considerably outperformed all baselines and the clinician policy, obtaining the highest estimated returns ($V = 21.73$). This suggests that the model learnt a superior policy which acts in accordance to high-return clinician actions while deviating from low return ones. Results of the external validation show consistent, albeit more modest results. The smaller improvements in the OPE returns on the AmsterdamUMC dataset may be explained by differences in patient populations (U.S vs European cohorts) and the differences in clinical setting/protocols, among other reasons.

2) *Mortality Rate*: In line with literature, we estimate mortality rates using the clinician policy's relationship between mortality and expected returns. We do this by categorizing expected returns from patient trajectories into bins and calculate the mortality rate for each bin. The resulting relationship between the expected returns and mortality is used to estimate mortality rates for learned policies based on their expected returns. The single-agent baselines (SoftAC-S and D3QN-S) showed approximate 26% and 22% increases in mean mortality rate compared to the clinician respectively, indicating a failure to learn an improved policy. In contrast, cooperative multi-agent baselines (QMix-O and QMix-T) showed a decrease of 12.2% and 21.7% in mortality rate. The non-cooperative multi-agent baselines (D3QN-O and D3QN-T) outperformed single agent baselines, but were less effective than the cooperative multi-agent baselines, highlighting the importance of collaboration among agents to obtain superior policies. Our model had the highest decrease in mean mortality by 38.9%, highlighting its ability to learn a policy that could considerably improve patient survival compared to state-of-the-art models and clinician policy. While we see a relatively smaller improvement in mortality rate in our external validation (20.9% decrease), our proposed model still achieves the lowest estimated mortality rate among all baselines, supporting the performance advantages of our approach.

3) *Mortality vs. Expected Return*: We further evaluate the efficacy of the learned policies by analyzing the correlation between mortality and expected returns (see Figure 2). An effective policy should display a strong negative correlation, where higher expected returns translate to lower mortality, and low expected returns to higher mortality. This relationship reflects the policy's ability to discern optimal actions from sub-optimal actions. The multi-agent baselines (QMix-O and QMix-T) display steeper negative curves than the single-agent baselines (D3QN-S and SoftAC-S). However, overall we see that none of the baselines consistently maintained the negative correlation throughout the plot—with plateauing and

positive correlations at some points in the plot. In contrast, the proposed model showed the steepest negative correlation with a consistent negative relationship, indicating the highest ability to improve patient survival. In our external validation, we see the same consistent negative relationship, indicating a good degree of generalizability.

4) *Mortality vs. Difference in Recommended Dosage*: For each intervention, we analyzed the relationship between mortality rates, and the recommended dosage differences between clinician-administered and learned policies. We estimated this relationship by categorizing quantile-level dosage differences into bins and computing mortality rates of each bin. An effective policy should align with clinician dosages that resulted in low mortality ($x\text{-axis}=0$), and increasingly deviate from those associated with increasing mortality, ideally forming a 'U' or 'V'-shaped curve centered at 0.

We showcase the performance of our model against the best-performing single-agent (D3QN-S) and multi-agent (QMix-T) models (see Figure 3). See Appendix, Section *Experimental Results* for comparison across all baseline models. The single-agent model failed to achieve the desired V-shape for any treatment, indicating a failure to properly learn from the large action space. The multi-agent baseline shows comparatively better performance, again demonstrating the advantage of cooperative agents operating under factored action spaces. On the other hand, our proposed model most closely approximated the desired V-shaped relationship across treatments; these qualitative results were also adequately replicated in our external validation, highlighting decent generalizability of our trained model.

3.3.2 **RQ2: Do individual agents learn effective local policies?** To assess if the agents operating within localized state-action subspaces learn effective treatment policies, We analyzed the relationship between mortality rates and discrepancies between the clinician and each agent recommended dosages (see Figure 4). Across all three organ systems, we observe that most agents showcase the desired V shape. For example, the Vasopressors and S1 agents show steep increases in mortality when deviating from clinician dosages, showing the sensitivity of the interventions. Proposed model tend to match effective dosing and adaptively diverge in high-risk scenarios, which supports is clinical relevance. Importantly, the renal sub-agents only appear in individual and cross-organ coordination rows as they do not contribute to intra-organ mixtures. This was intentionally modeled as renal treatments were found mutually exclusive in clinical practice, where diuretics and dialysis are found to be applied at different severity levels and rarely administered together. Enforcing exclusivity improves training stability and better reflects real-world treatment logic and flexibility in the proposed framework.

3.3.3 **RQ3: How does the learned policy compare to the clinician policy in the multi-organ treatment decision context?** We further assess how our learned policy aligns with clinician behavior in multi-organ intervention contexts. Specifically, we compare the pairwise treatment correlations across six intervention types between the clinician and the proposed policy. These comparisons are stratified by SOFA-based patient severity (i.e., low, medium and high) and survival outcome (i.e., survived vs. deceased) (see Figure 5). Note that exact alignment with clinician practice is neither

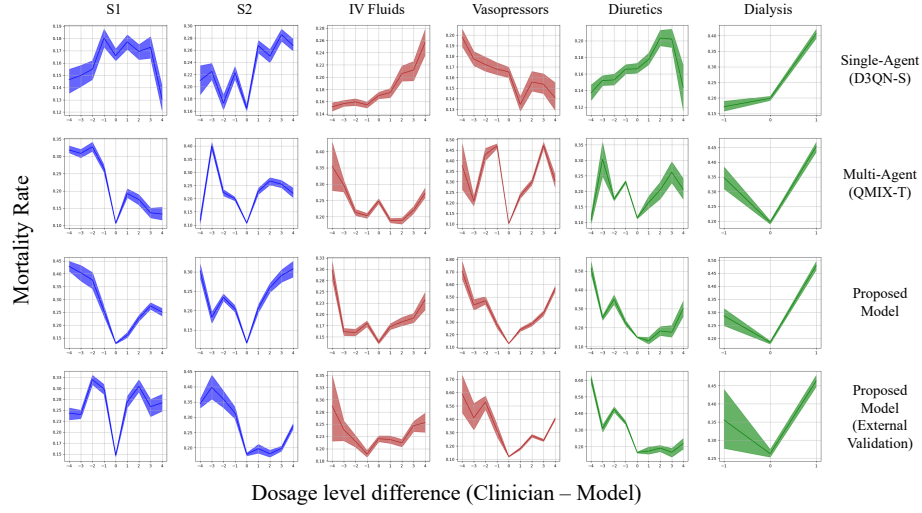


Figure 3: Dosage differences (x-axis) versus mortality (y-axis) for the top single-agent baseline SoftAC, multi-agent baseline QMix-T, proposed model on the testing set, and followed lastly by the proposed model on the external validation set, with colors blue, red, and green denoting different organ systems.

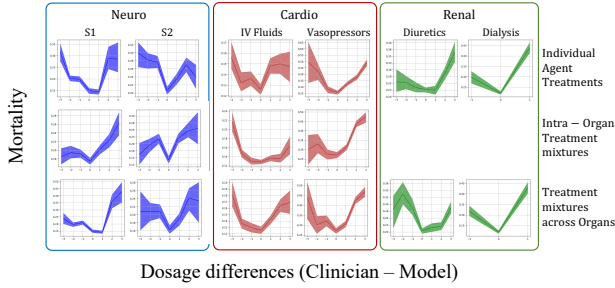


Figure 4: Mortality versus dosage difference (Clinician - Model) for individual agents across Neuro (blue), Cardio (red), and Renal (green) systems. Rows represent: individual treatments (top), intra-organ mixtures (middle), and inter-organ coordination (bottom). Renal agents do not include intra-organ mixtures due to clinical exclusivity between diuretics and dialysis.

expected nor optimal since it is well documented that clinicians often make suboptimal decisions under uncertainty in complex disease management. However, alignment with positive outcomes (i.e. survival) and divergence in high-risk cases (i.e., non-survivors) would showcase a robust and adaptive policy. It is evident that our policy closely replicated the positive treatment synergies observed in survivors across different severity levels, while showcasing reduced correlation with deceased cohorts. This indicates that the proposed model was able to recognize effective clinical patterns and also learned to avoid suboptimal treatment combinations associated with poorer outcomes. These findings showcase the policy’s ability

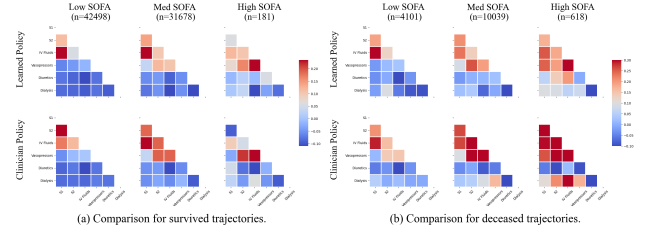


Figure 5: Correlation matrices of 6 treatment types within clinician and proposed policies across low, medium, and high SOFA severity levels, categorized by (a) survived and (b) deceased outcomes.

for adaptive decision-making based on patient state severity that could lead to superior outcomes.

3.3.4 RQ4: How effective are the proposed dual-layer state representations and cross-agent communication mechanisms?

We measured the contributions of two core components of our solution: dual-layer state representations and cross-agent communications. We trained three variations of our hierarchical model: without inter-agent communications (Prop-NoC), without the proposed state representations, using raw feature vectors (Prop-NoSR), and without (Prop-NoC-NoSR). All models showed degradation in mortality rates and CWPDIS values (see Tables 2 and 3). Compared to our full model, we see an increase of 27.2%, 19.7%, 33.4% in mean mortality for Prop-NoC, Prop-NoSR, and Prop-NoC-NoSR. These results demonstrate the critical role of these components.

Table 3: Off-policy evaluation metrics of the proposed model, without inter-agent communication and state representations.

Model	V	Mortality (%)
Prop-NoC	18.54	12.65 \pm 0.27
Prop-NoSR	19.01	11.92 \pm 0.36
Prop-NoC-NoSR	16.18	13.27 \pm 0.31

4 Conclusions

We introduce a hierarchical multi-agent reinforcement learning framework for the complex and first-of-its-kind multi-organ treatment recommendations, setting a new benchmark in clinical decision support systems. Mimicking real world collaborative clinical settings, our solution effectively decomposes the complex treatment process into a clinically meaningful hierarchy of subtasks. Each subtask is managed by specialized agents operating within dedicated subspaces. It supports independent and cooperative agent functionality through robust inter-and intra- organ communications. Moreover, a dual-layer state representation technique is proposed to support advanced contextualization needed at multiple levels in the hierarchy. We evaluate our solution on the non-standardized and multi-dimensional sepsis treatment recommendation problem. Comprehensive quantitative and qualitative evaluation on internal and external validation datasets showed that our solution consistently outperformed baselines, significantly improving the patient survival and effectively managing task complexity. Furthermore, learned policy closely followed successful clinical treatment patterns, deviating only when beneficial, thus enhancing the reliability of the policy. The inherent flexibility and scalability of our solution allow it to be expanded to a broader range of treatments and organ, and also for complex scenarios beyond healthcare.

References

- [1] Mohammad Asim, Farhana Amin, and Ayman El-Menyar. 2020. Multiple organ dysfunction syndrome: Contemporary insights on the clinicopathological spectrum. *Qatar medical journal* 2020, 2 (2020), 22.
- [2] Pooja Bhadoria and Harsha Rathore. 2021. Multi-organ system dysfunction in Covid-19-a review. *J Evolution Med Dent Sci* 10 (2021), 632–7.
- [3] Giacomo Deferrari, Adriano Cipriani, and Edoardo La Porta. 2021. Renal dysfunction in cardiovascular diseases and its consequences. *Journal of nephrology* 34, 1 (2021), 137–153.
- [4] Elisabetta Greco, Enrico Lupia, Ornella Bosco, Barbara Vizio, and Giuseppe Montrucchio. 2017. Platelets and multi-organ failure in sepsis. *International journal of molecular sciences* 18, 10 (2017), 2200.
- [5] Tuomas Haarnoja, Aurick Zhou, Pieter Abbeel, and Sergey Levine. 2018. Soft actor-critic: Off-policy maximum entropy deep reinforcement learning with a stochastic actor. In *International conference on machine learning*. PMLR, 1861–1870.
- [6] Alistair Johnson, Lucas Bulgarelli, Tom Pollard, Steven Horng, Leo Anthony Celi, and Roger Mark. 2020. Mimic-iv. *PhysioNet*. Available online at: <https://physionet.org/content/mimiciv/1.0/> (accessed August 23, 2021) (2020), 49–55.
- [7] Jaspreet Kaur and Prabpreet Kaur. 2024. A systematic literature analysis of multi-organ cancer diagnosis using deep learning techniques. *Computers in Biology and Medicine* 179 (2024), 108910.
- [8] Mohammad Shahbaz Khan, Rohit R Dixit, Anurima Majumdar, Valli Madhavi Koti, Sushant Bhushan, and Vipul Yadav. 2023. Improving Multi-Organ Cancer Diagnosis through a Machine Learning Ensemble Approach. In *2023 7th International Conference on Electronics, Communication and Aerospace Technology (ICECA)*. IEEE, 1075–1082.
- [9] Matthieu Komorowski, Leo A Celi, Omar Badawi, Anthony C Gordon, and Aldo Faisal. 2018. The artificial intelligence clinician learns optimal treatment strategies for sepsis in intensive care. *Nature medicine* 24, 11 (2018), 1716–1720.
- [10] Matthew C Konerman, David A Bozaan, Sarah Adie, Michael Heung, Jessica Guidi, Adam B Stein, Megan Mack, Dave Wesorick, and April Proudlock. 2022. Michigan Medicine Inpatient Diuretic Guideline for Patients with Acute Decompensated Heart Failure. (2022).
- [11] Yuki Kotani, Annamaria Di Gioia, Giovanni Landoni, Alessandro Belletti, and Ashish K Khanna. 2023. An updated “norepinephrine equivalent” score in intensive care as a marker of shock severity. *Critical Care* 27, 1 (2023), 29.
- [12] Siqi Liu, Kay Choong See, Kee Yuan Ngiam, Leo Anthony Celi, Xingzhi Sun, and Mengling Feng. 2020. Reinforcement learning for clinical decision support in critical care: comprehensive review. *Journal of medical Internet research* 22, 7 (2020), e18477.
- [13] Zhuo Liu, Linong Ji, Xuehan Jiang, Wei Zhao, Xiyang Liao, Tingting Zhao, Siqi Liu, Xingzhi Sun, Gang Hu, Mengling Feng, et al. 2020. A deep reinforcement learning approach for type 2 diabetes mellitus treatment. In *2020 IEEE International Conference on Healthcare Informatics (ICHI)*. IEEE, 1–9.
- [14] Mary Lynn M McPherson et al. 2010. *Demystifying opioid conversion calculations: a guide for effective dosing*. American Society of Health-System Pharmacists Bethesda, MD.
- [15] Dilruk Perera, Siqi Liu, and Mengling Feng. 2023. Demystifying Complex Treatment Recommendations: A Hierarchical Cooperative Multi-Agent RL Approach. In *2023 International Joint Conference on Neural Networks (IJCNN)*. IEEE, 1–10.
- [16] Aniruddh Raghu, Matthieu Komorowski, Imran Ahmed, Leo Celi, Peter Szolovits, and Marzyeh Ghassemi. 2017. Deep reinforcement learning for sepsis treatment. *arXiv preprint arXiv:1711.09602* (2017).
- [17] Aniruddh Raghu, Matthieu Komorowski, and Sumeetpal Singh. 2018. Model-based reinforcement learning for sepsis treatment. *arXiv preprint arXiv:1811.09602* (2018).
- [18] Tabish Rashid, Mikayel Samvelyan, Christian Schroeder De Witt, Gregory Farquhar, Jakob Foerster, and Shimon Whiteson. 2020. Monotonic value function factorisation for deep multi-agent reinforcement learning. *Journal of Machine Learning Research* 21, 178 (2020), 1–51.
- [19] Suchi Saria. 2018. Individualized sepsis treatment using reinforcement learning. *Nature medicine* 24, 11 (2018), 1641–1642.
- [20] Vikram Thakur, Radha Kanta Ratho, Pradeep Kumar, Shashi Kant Bhatia, Ishani Bora, Gursimran Kaur Mohi, Shailendra K Saxena, Manju Devi, Dhananjay Yadav, and Sanjeet Mehariya. 2021. Multi-organ involvement in COVID-19: beyond pulmonary manifestations. *Journal of clinical medicine* 10, 3 (2021), 446.
- [21] Philip S Thomas. 2015. Safe reinforcement learning. (2015).
- [22] Patrick J Thorat, Jan M Peppink, Ronald H Driessen, Eric JG Sijbrands, Erwin JO Kompanje, Lewis Kaplan, Heatherlee Bailey, Jozef Kesecioglu, Maurizio Cecconi, Matthew Churpek, et al. 2021. Sharing ICU patient data responsibly under the society of critical care medicine/European society of intensive care medicine joint data science collaboration: the Amsterdam university medical centers database (AmsterdamUMCdb) example. *Critical care medicine* 49, 6 (2021), e563–e577.
- [23] Ye Ella Tian, Vanessa Cropley, Andrea B Maier, Nicola T Lautenschlager, Michael Breakspear, and Andrew Zalesky. 2023. Heterogeneous aging across multiple organ systems and prediction of chronic disease and mortality. *Nature medicine* 29, 5 (2023), 1221–1231.
- [24] Guangyu Wang, Xiaohong Liu, Zhen Ying, Guoxing Yang, Zhiwei Chen, Zhiwen Liu, Min Zhang, Hongmei Yan, Yuxing Lu, Yuanxu Gao, et al. 2023. Optimized glycemic control of type 2 diabetes with reinforcement learning: a proof-of-concept trial. *Nature Medicine* 29, 10 (2023), 2633–2642.
- [25] Dale F Whelehan, Kevin C Conlon, and Paul F Ridgway. 2020. Medicine and heuristics: cognitive biases and medical decision-making. *Irish Journal of Medical Science (1971-)* 189 (2020), 1477–1484.
- [26] XiaoDan Wu, RuiChang Li, Zhen He, TianZhi Yu, and ChangQing Cheng. 2023. A value-based deep reinforcement learning model with human expertise in optimal treatment of sepsis. *NPJ Digital Medicine* 6, 1 (2023), 15.
- [27] Tsukasa Yagi, Ken Nagao, Eizo Tachibana, Naohiro Yonemoto, Kazuo Sakamoto, Yasushi Ueki, Hiroshi Imamura, Takamichi Miyamoto, Hiroshi Takahashi, Hiroyuki Hanada, et al. 2021. Treatment With Vasopressor Agents for Cardiovascular Shock Patients With Poor Renal Function: Results From the Japanese Circulation Society Cardiovascular Shock Registry. *Frontiers in Medicine* 8 (2021), 648824.
- [28] Hua Zheng, Ilya O Ryzhov, Wei Xie, and Judy Zhong. 2021. Personalized morbidity management for patients with type 2 diabetes using reinforcement learning of electronic health records. *Drugs* 81 (2021), 471–482.

Table 6: List of model features

Category	Feature Name
Demographics (8)	Age, Shock index, SOFA, GCS, Weight, SIRS, Gender, Readmission
Vital signs (10)	HR, SBP, MBP, DBP, Resp, Temp., PaCO2, PaO2, PaO2/FiO2 ratio, SpO2
Lab values (21)	Albumin, pH, Calcium, Glucose, Hb, Magnesium, WBC, Creatinine, Bicarbonate, Sodium, Lactate, Chloride, Platelets, Potassium, PTT, AST, ALT, BUN, Ionised calcium, Total bilirubin, Base excess
Output events (2)	Fluid output (4 hourly), Total output
Ventilation & others (3)	Mechanical ventilation, FiO2, Timestep

Abbreviations- PTT: Partial Thromboplastin Time; SIRS: Systemic Inflammatory Response Syndrome; ICU: Intensive care unit; WBC: White blood cell; Temp.: Temperature; GCS: Glasgow Coma Scale; Resp.: Respiratory rate; HR: Heart rate; SBP: Systolic blood pressure; MBP: Mean blood pressure; DBP: Diastolic blood pressure; Hb: Hemoglobin

Table 4: Summary of treatments, clinical components, purposes, and number of samples per treatment

Organ System	Treatment	Clinical Components	Purpose	Samples
Neurological	S1	Propofol	Anesthesia	71,389
	S2	Fentanyl, Morphine	Analgesia (pain relief)	89,400
Cardiovascular	IV Fluids	Crystalloids, colloids, blood products (tonicity adjusted)	Hemodynamic support, hydration, electrolyte balance	269,672
	Vasopressors	Norepinephrine, Epinephrine, Dopamine, Vasopressin, Phenylephrine	Increase blood pressure; stabilize hemodynamics	55,591
Renal	Diuretics	Furosemide, Bumetanide	Reduce BP and edema; maintain fluid balance	17,279
	Dialysis	Active renal replacement therapy	Waste removal, support kidney function	7,135

A Methodology

A.1 RL Actions:

For each 4-hour window, we computed the total dosage for each treatment by multiplying its infusion rate with the overlapping duration, and adding any IV push volumes. Treatments with multiple drugs were converted into their standard equivalents (i.e., vasopressors into norepinephrine [11], S2 to fentanyl [14], and diuretics to furosemide [10]) (see Table 4). Thresholds used for action discretization can be found in Table 5.

A.2 RL States:

State variables were chosen based on clinical relevance and concurrent availability in the MIMIC-IV and AmsterdamUMC datasets (see Table 6). The data was aggregated into 4-hourly windows using mean or sum as appropriate. Missing values were imputed using the 'last-observation carried forward' method (LOCF). Binary features were normalized to -0.5 and 0.5, and normally and log-normally distributed features to 0-1 range.

Table 5: Action level thresholds (4-hourly doses)

Treatment	0	1	2	3	4
IV Fluids (ml)	0	0.00–56.17	56.17–227.50	227.50–530.93	>530.93
Vasopressor (µg/kg)	0	0.00–9.40	9.40–20.66	20.66–44.42	>44.42
S1 (mg/kg of propofol)	0	0.00–3.40	3.40–6.01	6.01–9.53	>9.53
S2 (µg/kg of fentanyl)	0	0.00–0.65	0.65–2.08	2.08–4.30	>4.30
Diuretics (mg of furosemide)	0	0.00–20.00	20.00–160.00	160.00–902.10	>902.10
Dialysis	Off	On	–	–	–

A.3 Training Process

We describe the overall training process in Algorithm 1.

Algorithm 1 Generalized Training Process for HMARL Treatment Dynamic Treatment Recommender Solution

Require:
 W : a set of organ systems {i.e., {Neu, Car, Ren}}
 S : learned state representations, $S = \{s_t^{Rt}, s_t^o \mid \forall o \in W\}$
 a_c : clinician's action discretized into D dosage levels
 r : reward signal
 A_{Rt}, A_o : action spaces for root and organ-specific agents

- 1: **Initialize:** $Q(s, a)$ for:
- 2: Root agent: M_{Rt}
- 3: Single-organ agents: M_o for all $o \in W$
- 4: Treatment-level agents: M_o^{treat} for all $o \in W, \forall treat \in A_o$
- 5: Mixed-treatment agents: M_o^{Mix} for all $o \in W$
- 6: Mixed-organ agents: M_{OMix}
- 7: **Step 1: Train the Root Agent M_{Rt}**
- 8: Input: s_t^{Rt} {Unified state representations}
- 9: Output: $a \in A_{Rt}$ where $A_{Rt} = \{A_{Rt}^0, A_{Rt}^{OMix}\} \cup \bigcup_{o \in W} A_o^o$
- 10: **Step 2: Train Single-Organ System Agents**
- 11: **for** $o \in W$ **do**
- 12: Train $M_o(s_t^o, a)$ on $a_c \in A_o$
- 13: Output: $a_o^{master} \in \bigcup_{i=1}^{|A_o|} a_o^{master_i}$
- 14: **for** $treat \in A_o \setminus A_o^{Mix}$ **do**
- 15: Train $M_o^{treat}(s_t^o, a)$ on $a_c \in A_o \setminus A_o^{Mix}$
- 16: Output: $a \in \bigcup_{d \in D} a_o^{treat,d}$
- 17: **end for**
- 18: Train $M_o^{Mix}(s, a)$ on $a_c \in A_o^{Mix}$, where:
- 19: $s = \text{concat}(s_t^o, a_o^{treat} \mid \forall treat \in A_o \setminus A_o^{Mix})$
- 20: Output: $a \in \bigcup_{(treat,d) \in |A_o| \times D} a_o^{treat,d}$
- 21: **end for**
- 22: **Step 3: Retrieve Single-Organ System Actions**
- 23: **for** $o \in W$ **do**
- 24: Select a_o^{master} from M_o
- 25: Retrieve $G_o = \{a_o^{treat1}, \dots, a_o^{treatn}\}$, where $n = |A_o|$
- 26: **end for**
- 27: **Step 4: Train the Mixed-Organ Agents using QMIX**
- 28: Agents: $M_{OMix}(s, a)$ and M_o^o for all $o \in W$
- 29: Input: $s = [s_t^y, G_y \mid \forall y \in W]$
- 30: Output: Mixture of treatments across organ systems: A_t^{OMix}
- 31: **Step 5: Phase-2 Training**
- 32: See Equation (1) for detailed updates

B Experiments

B.1 Mortality vs. Difference in Recommended Dosage:

See Figure 6 for remaining plots omitted from main text.

B.2 Ethical Considerations:

Similar to RL based Clinical Decision Support Systems (CDSSs) proposed in the literature for various diseases including sepsis management [9, 16, 19], our solution is a human in the loop CDSS; where clinicians could utilize the data driven decisions provided by the intelligent agents as auxiliary inputs before making the final recommendations. In addition to the final action recommendations from the CDSS, the $Q(s, a)$ values available for all possible actions (a) could be used to quantify and compare the quality of the available

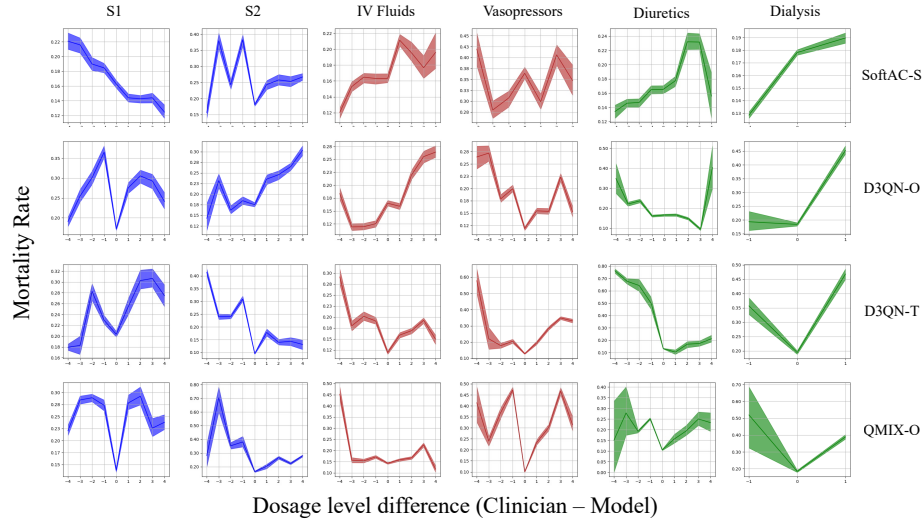


Figure 6: Baseline performances omitted due to space limitations from main text. Dosage differences (x-axis) versus mortality (y-axis) for individual agents in the hierarchy, with colors blue, red, and green denoting different organ systems.

treatment options for a given patient, with respect to his long term survival. The proposed solution allows clinicians to collaborate with the intelligent agent that combines the experiences of successful clinical decisions in the past, but leaves the full control of the final decision to the clinician. Furthermore, in line with the literature, all models were trained and evaluated using publicly available retrospective data, and no clinical trials were conducted. Therefore, the proposed solution does not raise ethical concerns.

B.3 Reproducibility and Model Parameters:

Source codes along with tuned parameters and architectures are uploaded with the submission and available online as an anonymous repository¹. All models are tested on the same holdout set. We experimentally set γ to 0.99 and k to 8. Data for the sepsis cohort can be replicated using the provided SQL scripts and Python codes.

Received 20 February 2007; revised 12 March 2009; accepted 5 June 2009

¹<https://anonymous.4open.science/r/HMARL-PyTorch-022B/>